VOL. 13, NO. 1, JANUARY 2018 ISSN 1819-6608
ARPN Journal of Engineering and Applied Sciences

www.arpnjournals.com

LANDAU THEORETICAL INTERPRETATION OF DOMAIN AND DOMAIN WALLS IN FERROELECTRIC FERROICS

Egidius Rutatizibwa Rwenyagila[1] and Stanley Ferdinand Mwanga[2]
[1]Department of Physics, University of Dar es Salaam, Dar es Salaam, Tanzania
[2]Department of Physics, University of Dodoma, Dodoma, Tanzania
E-Mail: egidiruta@yahoo.co.uk

ABSTRACT

In this paper some behaviors of domain and domain walls in perovskiteferroics were theoretically investigated. Landau type theory was used to examine the phenomenological properties of domains and domain walls in ferroelectric perovskite materials. Landau predictions on the prototype ferroelectric $BaTiO_3$showedthatithasa stable tetragonal structure at room temperature. The number of domains in the three ferroelectric phases of $BaTiO_3$wasalsocalculated. The results confirmed six, eight and twelve domain states in the tetragonal, rhombohedral and orthorhombic structures of $BaTiO_3$, respectively. The respective spontaneous polarization and domain wall thickness in the stable tetragonal $BaTiO_3$have values of 0.26 Cm^{-2} and 1.63 nmat room temperature. Analytical and numerical solutions for the relationship between temperature and domain wall thickness and for the spatial distribution of polarizations inside the domain wall are also determined and discussed.

Keywords: domain walls, ferroelectricity, Landau theory, symmetry.

INTRODUCTION

Landau theory is a phenomenological theory that was established in 1937 by Lev Davidovich Landau[1] in order to explain the concept of Curie point structural anomalies of physical properties that occur generally in second-order phase transitions[2]. The theory relates the macroscopic behavior of materials to the breaking of material symmetry along with the change in the order parameters and to the change in the so called Landau free-energy of phase transformations. The breaking of symmetry means that one or more symmetry elements of the crystal suddenly appear or disappear across the transition temperature of a given material[3]. As a consequence, after the transition region, the non-symmetric parent phase may be represented as distorted symmetrical phase and vice versa. In principle, the structural changes that occur at the transition point represent very important materials aspects that are usually sufficient for the description of anomalies in many practical thermodynamic properties of materials; thence forming the basis of the Landau theory.

Depending on the crystal structure and on the order parameters of particular materials, ferroelectricity, antiferroelectricity and ferroelasticity can usually occur when a material is cooled down from paraelectric or paraelasticcentro symmetric states through the transition temperatures (Tc). Because of this, the two (parent and daughter) phases will acquire different symmetries and domains and domain-walls can occur in the new structural states. The ferroelastic domains are typically designated as 90^o domains and the boundary between them as 90^o domain walls. In addition, 180° domains and domain walls occur in ferroelectric materials. Thus, in typical ferroelectric materials 180° domains and 90^o domains can be fully or partially coupled and/or totally uncoupled. Note that, in several ferroelastic and ferroelectric devices as well as in the characterization of ferroics, the 90° and 180° domain-walls play important roles in influencing the device performances and the general ferroics properties. For example, different researchers have shown that the presence and subsequent displacement of domain walls enable the control of dielectric loss mechanism in capacitors, electro-optic effects switching and provision of ferroics substrates for the deposition of high T_C superconductor films[4].

By definition, ferroics represent classes of materials whose properties are mainly derived from the crystallographic and physical properties of their structural phase transitions. Therefore ferroics form a group of important material candidates for domain and domain-wall engineering. Besides being good candidates for domain wall engineering, some ferroics, particularly lead-free ferroics present powerful toolboxes for the development of the so-called environmental friendly piezoelectric materials[5-7]. Such piezoelectric materials play important roles in wide range of technological devices and components. These include their remarkable applications as sensors, transducers and actuators that are integrated in a variety of multifunctional machineries ranging from biomedical instrumentation to energy structures, communication and information storage systems and other more.

Although the situation with the nucleation of domains is somehow complicated and ambiguous in most of its aspects, some techniques have been proposed[8]. These techniques demonstrated among other materials issues the enhancement of piezoelectric properties originating from engineered domain configurations and domain-wall engineering techniques. The major role in these techniques is played mainly by the anisotropy of the material, the defect structures as well as in homogeneities of sample structures[3] and of most important for ferroics is that domains arise almost in any phase transitions[8].

In connection with theoretical understanding of domains and domain-walls in ferroics, the Landau theory is undeniably a very useful tool[9].This is due mainly to

the fact that the Landau system of equations for an equilibrium order parameter relates the macroscopic behavior of materials to the breaking of their symmetries. Symmetry breaking is then represented by the change in the order parameter and the change in the Landau-free energy density of phase transformations (ΔG).This paper presents some theoretical analyses of domain and domain walls in perovskiteferroics. Landau type theory is used to study the phenomenological properties of domains and domain walls in ferroelectric perovskite materials.

DOMAIN STATES IN FERROELECTRIC PHASE TRANSITIONS

Certain materials known as ferroics acquire several low-temperature phases when they are cooled from their high temperature prototype cubic symmetry. Many of these materials include the most important functional perovskite materials, such as barium titanite ($BaTiO_3$) and lead zirconatetitanite (PZT) compositions. Ferroics phases are usually induced through atomic and structural displacement at the phase transitions. Because of atomic displacements some of thermally induced ferroics phases are usually associated with domain states, so that the stable structures of materials like $BaTiO_3$ depend on certain temperature ranges. As a natural rule, one looks for optimizing material properties at room conditions where most of our functional devices are likely to be subjected. Nevertheless, materials for high temperature and low temperature applications are important and require lot of their development. To this end, it is essential to know the conditions associated with stabilities of materials and the nature of domain structures that are occurring in materials during temperature induced phase transitions.

The problem of phase transitions and domain structure can be addressed by experiments or theoretical approaches and/or combination of the two. In a theoretical perspective the well-known Landau free-energy theory exists[10] and has been frequently used for various estimations and treatment of domain structures and domain wall properties in a wide range of materials[11].Landau-type phenomenological theory is derived from the Gibbs potential[12] and it has been shown to offer realistic tool for the understanding of qualitative and quantitative physical properties during temperature and/or field induced phase transformations[9,13].

Landau theory has also been successful in explaining the properties of domain states[14]and structural properties in a temperature induced phase transitions in the absence of field and/or stress[15]. In this prominent phenomenological theory the so-called Landau potential functional is usually written in different ways that allow for number of physical quantities such as spontaneous polarizations of single-domain states to be obtained in form of very simple explicit equations. In what follows, the problem of the domain states and domains structures of the most prominent perovskiteferroicsis examined. In parallel the spontaneous polarizations and stability of the ferroelectric low-temperature phases are discussed within the frame-work of Landau-type continuum theory.

Landau-type functional of domain states

Landau-Ginsburg-Devonshire phenomenological theory of phases expresses the free-energy density difference between the actual ferroelectric state and the hypothetical cubic state as power series of order parameter (polarization) and strain under isothermal conditions[10]. Generally, any homogeneous system at equilibrium state in an applied homogeneous stress and electric field can be expressed by the Gibbs free-energy density given by:

$$\Delta G_{(T,\sigma,\vec{E},X,\vec{P})} = G_L + G_C + G_q - \sigma X - \vec{E}\vec{P} \quad (1)$$

where G_L, G_C, G_q and σX are the respective Landau, coupling, electrostrictive and stress energy terms, $\vec{P}$ is the polarization and $\vec{E}$ is the electric field. This is a phenomenological theory in which the dependence of the free-energy density on strain is expressed by introducing a bilinear elastic and electrostriction tensors abbreviated by Voigt suffixes *i=1-6*such that (*1=11, 2=22, 3=33, 4=23, 5=13* and *6=12*). Under zero field condition, a part of the general Gibbs free-energy density is left behind and the remaining part is expanded to give:

$$\begin{aligned}\Delta G &= \alpha_1(P_1^2+P_2^2+P_3^2)+\alpha_{11}(P_1^4+P_2^4+P_3^4)\\ &+\alpha_{12}(P_1^2P_2^2+P_2^2P_3^2+P_3^2P_1^2)+\alpha_{111}(P_1^6+P_2^6+P_3^6)\\ &+\alpha_{112}[P_1^4(P_2^2+P_3^2)+P_2^4(P_1^2+P_3^2)+P_3^4(P_1^2+P_2^2)]\\ &+\alpha_{123}(P_1^2P_2^2P_3^2)-0.5s_{11}(X_1^2+X_2^2+X_3^2)\\ &-s_{12}(X_1X_2+X_2X_3+X_3X_1)-0.5s_{44}(X_4^2+X_5^2+X_6^2)\\ &-Q_{11}(X_1P_1^2+X_2P_2^2+X_3P_3^2)-Q_{12}[X_1(P_2^2+P_3^2)+X_2(P_1^2+P_3^2)\\ &+X_3(P_1^2+P_2^2)]-Q_{44}(X_4P_2P_3+X_5P_1P_3+X_6P_1P_2)\end{aligned} \quad (2)$$

where $P_i$andX_i are polarization and stress parameters. α_i,$\alpha_{ij}$and $\alpha_{ijk}$are stiffness and high-order stiffness coefficients at constant stress. s_{ij}Isthecoefficient of elastic compliance at constant polarization and$Q_{ij}$is the cubic electrostrictive constant. In the case of symmetric displacive transformations occurring in perovskiteferroics of $BaTiO_3$-type the role of order parameter is usually played by the spontaneous polarizationP_i where$i = 1, 2, 3$ represents the 3 prominent Cartesian components.

To be classified as ferroelectric ferroics a material needs to possess more than one stable polarization orientation states in the absence of electric field and mechanical stress but the states can be reoriented in one of its states by means of applied electric field, stress or combination of the two. This implies that under the condition of free-stress and absence of electric field, only homogeneous spontaneous strain or polarization is expected to occur inferroelectric materials. Under such conditions the Gibbs free-energy density reduces to the Landau-type free-energy density functional. It is given by

$$\Delta G_{Landau} = \Delta G(X = E = 0) \quad (3)$$

The resulting Landau-type free energy functional is usually written as the systematic-expansion of the cubic invariant rotational symmetry in terms of given materials order parameters. For example, to understand the nature of domain states and phase transition occurring in $BaTiO_3$-type perovskites, one requires a Landau-free energy density functional model with terms up to at least sixth power of polarization components. This is given by:

$$\Delta G = \alpha_1(P_1^2 + P_2^2 + P_3^2) + \alpha_{11}(P_1^4 + P_2^4 + P_3^4) + \alpha_{12}(P_1^2P_2^2 + P_2^2P_3^2 + P_3^2P_1^2) + \alpha_{111}(P_1^6 + P_2^6 + P_3^6) + \alpha_{112}[P_1^4(P_2^2 + P_3^2) + P_2^4(P_1^2 + P_3^2) + P_3^4(P_1^2 + P_2^2)] + \alpha_{123}P_1^2P_2^2P_3^2 \quad (4)$$

The solution to this form of Landau-type equation is used to estimate for example most of the properties of single-domain state materials like $BaTiO_3$. That is to say, in such a model the number of physical quantities such as spontaneous polarization and the corresponding free-energy density need to be derived and expressed as simple expressions. The possible symmetric transformation solutions corresponding to equation (4)for perovskiteferroics were reported earlier by different scholars[10, 11]. For example, solutions of the three ferroelectric phases of $BaTiO_3$from literature are presented in Table-1.

Table-1. Polarization symmetries of$BaTiO_3$ferroelectric phases [10, 11].

Phase	Crystal	Symmetry	Polarization states	Polar direction
0	Cubic	m3m	$P_1^2 = P_2^2 = P_3^2 = 0$	paraelectric
I	Tet	4mm	$P_1^2 = P_2^2 = 0, P_3^2 \neq 0$	$\langle 001 \rangle$
II	Ort	mm2	$P_1^2 = P_2^2 \neq 0, P_3^2 = 0$	$\langle 101 \rangle$
III	Rho	3m	$P_1^2 = P_2^2 = P_3^2 \neq 0$	$\langle 111 \rangle$

Spontaneous polarization of tetragonal $BaTiO_3$

When the values of Table-1 are combined with Landau-type functional (equation 4), the spontaneous polarizations corresponding to the hypothetical cubic phase and three ferroelectric phases of $BaTiO_3$ are readily determined. The free energy density of the cubic structure turns out to be zero. This indicates that the cubic structure is paraelectric (Table-1). It also explains the reason why cubic phase is usually taken as the reference phase.With free energy density of zero in cubic phase, the other phases occurring in perovskites of $BaTiO_3$-type can be referred to it. The corresponding Landau-free energy density of the tetragonal phase is given by:

$$\Delta G = \alpha_1 P_3^2 + \alpha_{11} P_3^4 + \alpha_{111} P_3^6 \quad (5)$$

Minimization of equation (5) leads to:

$$\left(\frac{\partial(\Delta G)}{\partial \Delta P_3}\right)_{P_3 = P_s} = \alpha_1 + 2\alpha_{11}P_3^2 + 3\alpha_{111}P_3^4 = 0 \quad (6a)$$

or equivalently to,

$$P_s = \sqrt{\frac{-\alpha_{11} + (\alpha_{11}^2 - 3\alpha_1\alpha_{111})^{1/2}}{3\alpha_{111}}} \quad (6b)$$

Table-2 presents the numerical expansion coefficients of the Landau-type free energy density for the case of $BaTiO_3$. The parameters are usually estimated from different combinations of both experimental and theoretical findings[11, 12]. Although Landau expansion parameters may sometimes fail to describe some higher-order effects, hence, leading to insufficient precision of the estimated values[14]. In most cases the discrepancies have been shown to be insignificantly very small and most phenomenological predictions basing on these parameters have been shown to be in good agreement with actual experimental results[10-12].Combining expansion parameters (Table-2) and equation (6), the magnitudes of spontaneous polarization in tetragonal $BaTiO_3$ and other perovskites undergoing $BaTiO_3$-type structural phase transitions can be obtained.

Table-2. Different $BaTiO_3$Landau-Ginsburg-Devonshire polynomial coefficients.

Coefficients	Li *et al.* T (°C) [12]	Bell and Cross T (°C) [11], [12]
α_1 (VmC^{-1})	4.124×10^5(T-115)	3.34×10^5(T-108)
α_{11} (Vm^5C^{-3})	-2.097×10^8	4.69×10^6(T-120)-2.02×10^8
α_{12} (Vm^5C^{-3})	7.974×10^8	3.23×10^8
α_{111} (Vm^9C^{-5})	1.294×10^9	-5.52×10^7(T-120)$+2.76\times10^9$
α_{112} (Vm^9C^{-5})	-1.950×10^9	4.47×10^9
α_{123} (Vm^9C^{-5})	-2.500×10^9	4.91×10^9
α_{1111} ($Vm^{13}C^{-7}$)	3.863×10^{10}	-
α_{1112} ($Vm^{13}C^{-7}$)	2.529×10^{10}	-
α_{1122} ($Vm^{13}C^{-7}$)	1.637×10^{10}	-
α_{1123}($Vm^{13}C^{-7}$)	1.367×10^{10}	-

Nevertheless, even before assessment of the spontaneous polarization (P_S) magnitudes in the three ferroelectric phases of $BaTiO_3$ the first direct insightful impression one gets is that $BaTiO_3$ and other displacive perovskiteferroics show no spontaneous polarization in their cubic phases. On the other hand, from equation (6) one finds that tetragonal phase is ferroelectric with non-zero net polarization. Since polarization is not zero, in the tetragonal phase the number of domains and tetragonal domain structure usually referred to as ferroelectric domain states can also be explicitly determined. For the purpose of predicting the phase transitions and determination of ferroelectric properties of materials such as domain structures most scholars often assume a linear temperature dependence of the dielectric stiffness α_1[10-12]. This assumption is derived from the Curie-Weiss law given by:

$$\alpha_1 = \left(\frac{T-T_0}{\varepsilon_0 C}\right) \quad (7)$$

where $\varepsilon_0$is the permittivity of the free space, 8.8542×10^{-12} Fm^{-1}. For the bulkcrystal of $BaTiO_3$ the values of Curie constant, C of ~ 1.5×10^5 °C and Curie-Weiss temperatureT_0rangingbetween 108 -115 °C have been reported[15].However, in a real physical system the coefficients of Landau-type expansion should generally depend on the entire set of the thermodynamic state variables including temperature. The relationship of the temperature dependent coefficient was reported earlier by Bell and Cross[11,12] (Table-2). Using their formulae the temperature dependent coefficients corresponding to room temperature $BaTiO_3$structure have been recalculated and the values obtained are presented in Table-3.

Moreover, the magnitudes of C and T_0 in equation (7) as well as the other parameters of Landau-type theory largely depend on the definition of the relevant conditions used during materials synthesis and processing. Therefore, in order to avoid some inconsistencies arising from polycrystalline materials, it is usually convenient to estimate the value of $\alpha_1$and the other Landau-type expansion parameters (Table-3) only from the bulk-single crystal materials such as $BaTiO_3$ at specified ambient conditions. The value of $\alpha_{11} < 0$ (Table-3) indicates that the transformation phenomenon described is of first-order type. Adding the values of Table 3 into equation (6b), one readily obtains the value of spontaneous polarization P_s in a tetragonal $BaTiO_3$ structural phase. It is 0.26 Cm^{-2}. This magnitude of polarization corresponds well to the room temperature polarization values of ferroelectric tetragonal barium titanite obtained from other sources.

Table-3. The room temperature Landau-type expansion coefficients used in the prediction of P_s in $BaTiO_3$.

Coefficient	α_1(VmC^{-1})	$\boldsymbol{\alpha_{11}}$(Vm^5C^{-3})	$\boldsymbol{\alpha_{111}}$($Vm^9C^{-5}$)
Magnitude	-3.006×10^7	-6.4755×10^8	8.004×10^9

Features of ferroelectricity in tetragonal phase

The obtained spontaneous polarization of 0.26 Cm^{-2} proves the well-known ferroelectricity of tetragonal $BaTiO_3$.The origin of ferroelectric properties in tetragonal $BaTiO_3$structure can be attributed to its structure. Principally, $BaTiO_3$ transforms to tetragonal modification at its transition temperature around 120°C. At this point displacements of the Ti and oxygen ions from their symmetry sites of the paraelectric cubic phase occur. As a consequence, the movement of ions cause competitions between covalent and ionic forces involving Ti and O and result to changes in the Ti-O bond lengths. It has been reported that the competition produces six bonds of varying lengths categorized as short bonds that vary between *1.83–1.90* Å, intermediate bonds varying within $2.00 - 2.03$ Å and long bonds in the order of*2.11–*

*2.21*Å [13].The bond properties for tetragonal, orthorhombic, and rhombohedral structures can easy be visualized in the illustration (Figure-1).

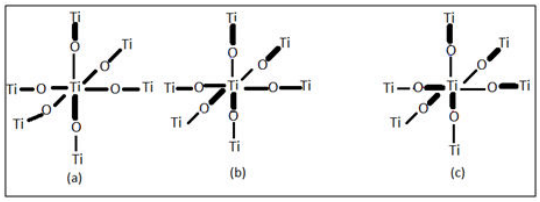

Figure-1. Graphical representation of the nearest location of a titanium atom in (a) tetragonal, (b) orthorhombic, and (c) rhombohedral phases of $BaTiO_3$[13]. The thickest lines, thicker lines and thinner lines in the sketch represent short, intermediate and long bonds, respectively.

This illustrates the environment of titanium, the three types and/or the number of Ti-O bond lengths corresponding to the three ferroelectric phases of barium titanate. Note that tetragonal $BaTiO_3$ is described by TiO^{2+} groups that upon bounding strongly with each other result to strong interaction that orients ultimately the Ti-O adjoined chains along one given tetragonal direction. Because of the polarities of Ti-O bonds the orientation of TiO^{2+} chains reorients the dipole moments of the same Ti-O bonds and results to spontaneous polarization as a result of dipole moment per unit volume. The resulting bond distances (Table-4) in the tetragonal structure are in such a way that one bond is long, the other one becomes short and the rest are between normal and intermediate bonds. This effect of bond length variations along with the orientations of Ti-O dipoles result to both ferroelectricity and tetragonal structure of $BaTiO_3$ with space group of *P4mm*and unit-cell parameters of (*a, c*) = (3.99095, 4.0352) Å at room temperature[13].

Table-4. Ti-O bond lengths and their numbers in $BaTiO_3$ferroelectric phases[13].

Phases	T, K	Type of bond					
		Short		Intermediate		Long	
		Length, Å	N°	Length, Å	N°	Length, Å	N°
Rho	132	1.890	3	-	-	2.122	3
	130	1.874	3	-	-	2.136	3
Ort	263	1.90	2	2.00	2	2.11	2
	270	1.863	2	1.999	2	2.157	2
Tet	295	1.877	1	2.001	4	2.166	1
	295	1.862	1	2.030	4	2.172	1
	298	1.860	1	2.002	4	2.174	1
	298	1.87	1	2.004	4	2.15	1
	300	1.829	1	2.000	4	2.206	1

Ferroelectric domain states in tetragonal $BaTiO_3$

During ferroelectric phase transition from a parent phase *G* to a new distorted phase *F*, domains can occur in certain displacive materials. The determination of the number of domain states *q* (also known as index of phase*F* in phase*G*) is based generally on symmetry operations of the parent or reference state *G*. This is given by[9]:

$$q = \frac{|G|}{|F|} \quad (8)$$

where$|G|$ and$|F|$are the respective order of the point groupsof parent phase and the daughter phase (Table-5)given by the number of structural symmetry operations and identity transformations. The values of $|G|$ or $|F|$also known as order of the group are obtained directly from the well-known 32 point groups of crystals[9]. The possible point groups that correspond to the three ferroelectric phases of $BaTiO_3$ are shown in Table 5along with numbers of their corresponding domain states and crystal class systems. Following the notation of Tagantsev *et al.*[9]ferroics species can be denoted according to the transitions they represent. This ultimately allows the inclusion of all newly attained phase transition properties between the symmetries of parent phase *G* and the daughter phase *F*. For example, the species of the form:$G - P\varepsilon ds - F$ represents a phase transition that shows ferroelectric (*P*), ferroelastic (ϵ), ferroelastoelectric (*d*) and ferrobielastic (*s*) occurring all together in such a particular phase transition. With this notation and in the case of displacive $BaTiO_3$, one becomes interested in the prominent ferroelectric phase transition characterized by the species of the form$m\bar{3}m - P\varepsilon ds - 4mm$.

Table-5. Symmetric point groups, transition temperatures and number of domain states in ferroelectric phases of $BaTiO_3$[9].

Phase	0 Paraelectric	I Ferroelectric	II Ferroelectric	III Ferroelectric
	Cubic (G)	**Tet** (F)	**Ort** (F)	**Rho** (F)
Symmetry	$m\bar{3}m - O_h$	$4mm - C_{2v}$	$mm2 - C_{2v}$	$3m - C_{3v}$
Ordergrp	48	8	4	6
Domains	q = G/F	6	12	8
T_C(°C)	120	5	-90	

For simplicity only ferroelectric *(P)* properties of the species have been considered. Thus, in a general case being a multi-axial ferroelectric material, $BaTiO_3$ can show more than one ferroelectric species namely$m\bar{3}m - P\varepsilon ds - mm2$, $m\bar{3}m - P\varepsilon ds - 3mandm\bar{3}m - P\varepsilon ds - 4mm$[9]. However, one finds that for the case of first-order the important species is the one described by $m\bar{3}m - P\varepsilon ds - 4mm$thatresults to the stable tetragonal $BaTiO_3$with point group of*4mm*.Accordingly and in line with Landau-type phenomenological theory, one readily finds that the *4mm* tetragonal phase contains six number of ferroelectric domain states. These states are obtained directly using equation (8) and the group order values presented in Table5. Similar calculation of the number of domain states for the other two ferroelectric phases of $BaTiO_3$ reveals that there are 12 domain states in the orthorhombic phase and 8 domain states in the rhombohedral phase. Both data and the calculated number of domain states for the ferroelectric phases of $BaTiO_3$ are presented in Table-5.Figure-2 presents polarization in terms of its Cartesian components, the six domain states in tetragonal$BaTiO_3$ are marked by the states$(0, \mp P_S, 0)$, $(0,\ 0, \mp P_S)$and $(\mp P_S, 0, 0)$. Thus, the order parameter gives the measure of spontaneous polarization indicated by arrows that equivalently gives the measure of the displacement of the atoms from their paraelectric cubic positions.

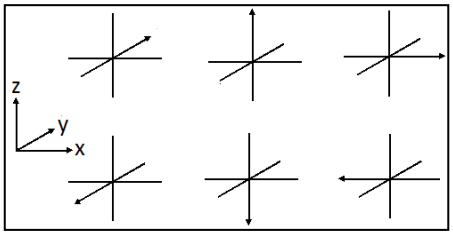

Figure-2. Possible orientations of domain states in the tetragonal phase of barium titanite.

Stability of ferroelectric phases of $BaTiO_3$

Based on the free energy density, the stability of the three ferroelectric phases of barium titanite at room temperature can be compared. Using the value of spontaneous polarizations and the specific free-energy density expressions of each ferroelectric phase, the change in free energy densities of tetragonal, orthorhombic and rhombohedral $BaTiO_3$can be calculated and their structural phase stabilities at room temperature can be evaluated. In the case of tetragonal $BaTiO_3$, when the value of the calculated spontaneous polarization, P_s = *0.26* Cm^{-2} is used into equation (5) the change in free energy density obtained for room temperature is – 2.5 $MVCm^{-3}$. If the values of Table 1 for the orthorhombic phase are also used into equation (4), the expression for the change in free energy density is given by:

$$\Delta G = \alpha_1(P_1^2 + P_2^2) + \alpha_{11}(P_1^4 + P_2^4) + \alpha_{12}P_1^2P_2^2 + \alpha_{111}(P_1^6 + P_2^6) + \alpha_{112}[P_1^4P_2^2 + P_2^4P_1^2] \quad (9a)$$

or equivalently,

$$\Delta G = (2\alpha_1P_S^2 + 2\alpha_{11}P_S^4 + \alpha_{12}P_S^4 + 2\alpha_{111}P_S^6 + 2\alpha_{112}P_S^6)_{P_1=P_2=P_S} \quad (9b)$$

To deduce the magnitude of spontaneous polarization one needs to find the minimum of the orthorhombic free energy density functional from equation (9) such that

$$\frac{\partial(\Delta G)}{\partial P_S} = 4\alpha_1P_S + 8\alpha_{11}P_S^3 + 4\alpha_{12}P_S^3 + 12\alpha_{111}P_S^5 + 12\alpha_{112}P_S^5 = 0 \quad (10a)$$

or equivalently,

$$P_S^2 = \frac{-(2\alpha_{11} + \alpha_{12}) + \sqrt{(2\alpha_{11} + \alpha_{12}) - 12(\alpha_{111} + \alpha_{112})\alpha_1}}{6(\alpha_{111} + \alpha_{112})} \quad (10b)$$

Following Bell and Cross[11,12]proposition (Table-2) the values of the Landau-type expansion parameters corresponding to the room temperature (25°C) can be recalculated for orthorhombic phase transition occurring at about 5°C. These are presented in Table-6. Combining Table-6 and equation (10b) the spontaneous polarization, P_s of 0.19 $Cm^{-2}$for orthorhombic is obtained. This value corresponds to the room temperature equilibrium polarization $(P_1 = P_2 = P_S)$ values in a ferroelectric orthorhombic barium titanite phase. Inserting P_s value into equation (9) the average change in free energy density corresponding to orthorhombic barium titanite at room temperature is also obtained. It is -1.5 $MVCm^{-3}$.

Table-6. Landau-type free-energy expansion coefficients for orthorhombic $BaTiO_3$.

Coefficient	Tetrag phase[11, 12]	Ort calculated
α_1VmC^{-1}	3.34×10^5(T-108)	-3.006×10^7
α_{11}Vm^{5}C^{-3}	4.69×10^6(T-120)-2.02×10^8	-1.082×10^8
α_{12} Vm^{5}C^{-3}	3.23×10^8	3.23×10^8
α_{111}Vm^{9}C^{-5}	-5.52×10^7(T-120)+2.76×10^9	1.656×10^9
α_{112}Vm^{9}C^{-5}	4.47×10^9	4.47×10^9

Now assuming that rhombohedral phase appears at room temperature, in this case the solution to the Landau phenomenological functional takes the form of$P_1^2 = P_2^2 = P_3^2 \neq 0$. Equation (4) can be rewritten using this polarization symmetry states to represent the change in free-energy density associated to rhombohedral $BaTiO_3$. This turns out to be:

$$\Delta G = 3\alpha_1 P_S^2 + 3P_S^4(\alpha_{11} + \alpha_{12}) + P_S^6(3\alpha_{111} + 6\alpha_{112} + \alpha_{123}) \quad (11)$$

As for the case of tetragonal and orthorhombic states, equation (11) has to be minimized in order to estimate the magnitude of spontaneous polarization $P_s$in the structure of rhombohedral $BaTiO_3$. Minimization gives:

$$\frac{\partial(\Delta G)}{\partial P_s} = 6\alpha_1 P_S + 12P_S^3(\alpha_{11} + \alpha_{12}) + 6P_S^5(3\alpha_{111} + 6\alpha_{112} + \alpha_{123}) = 0 \quad (12a)$$

or equivalently,

$$P_S^2 = \frac{-2(\alpha_{11} + \alpha_{12}) + \sqrt{(2(\alpha_{11} + \alpha_{12}))^2 - 4(3\alpha_{111} + 6\alpha_{112} + \alpha_{113})\alpha_1}}{2(3\alpha_{111} + 6\alpha_{112} + \alpha_{113})} \quad (12b)$$

If the rhombohedral transition temperature of -90^{o}C is taken into account the values of coefficients for rhombohedral $BaTiO_3$ are calculated. The results are presented in Table-7.

Table-7. Coefficient values of the Landau-type functional in rhombohedral $BaTiO_3$.

Landau coefficient	Value
α_1VmC^{-1}	-3.006×10^7
α_{11}Vm^{5}C^{-3}	3.3735×10^8
α_{12}Vm^{5}C^{-3}	3.23×10^8
α_{111}Vm^{9}C^{-5}	-3.588×10^9
α_{112}Vm^{9}C^{-5}	4.47×10^9
α_{113}Vm^{9}C^{-5}	4.91×10^9

Combining Table-7 and equation (12b) yields the value of spontaneous polarization P_s = *0.13 Cm^{-2}* corresponding to the rhombohedral $BaTiO_3$ at room temperature. The change in free-energy density for the rhombohedral phase can now be easily estimated using the obtained spontaneous polarization P_S into equation (11). This turns out to be -0.9 MVCm^{-3}.

While it can be contended that, the predicted free energy densities are not the exact physical energy figures of the three ferroelectric states of barium titanite, the trend $(\Delta G_{Tet} \sim -2.5 < \Delta G_{Ort} \sim -1.5 < \Delta G_{Rho} - 0.9)$MVCm^{-3} so far represents an important theoretical inference. It suggests that at room temperature orthorhombic and rhombohedral phase are absolutely unstable with their energies corresponding to energy maxima. From Landau-type phenomenological theory in agreement with the obtained free energy density values, one is sure that at room temperature tetragonal is the stable structural phase of $BaTiO_3$. Therefore at room temperature $BaTiO_3$ occurs in a tetragonal form with its six domain states (Table-5 and Figure-2).

Second order phase transition

In most ferroics both first order and second order phase transitions can occur[9]. If the phase transition is second order, one starts with Landau-type free energy density functional of tetragonal phase (equation 4) and sets $\alpha_{11} > 0$ and $\alpha_{111} = 0$. Landau thermodynamic free energy density function can then be written to represent second order phase transition. It is given by:

$$\Delta G = \alpha_1 P_3^2 + \alpha_{11} P_3^4 \quad (13)$$

By minimizing the free energy density in equation (13) a new Landau-type thermodynamic expression with variable in the form of rescaled units is obtained. This is given by:

$$\frac{\partial(\Delta G)}{\partial P_3} = 2\alpha_1 P_3 + 4\alpha_{11} P_3^3 = 0 \quad (14)$$

Since there is no any applied external electric field, for a ferroelectric phase transition at conditions$T < T_0$ the solution of equation (14) shows the occurrence of spontaneous polarizationgiven by:

$$P_3^2 = \pm P_S^2 = \frac{-\alpha_1}{2\alpha_{11}} \quad (15a)$$

or equivalently,

$$P_S^2 = \frac{\alpha_0(T_0 - T)}{2\alpha_{11}} \text{ (if Curie-Weiss law is used)} \quad (15b)$$

When the Curie-Weiss law is used to replace the stiffness coefficient $\alpha_1$in equation (13) the temperature variation of polarization is introduced, and a new Landau thermodynamic energy density is obtained. It is:

$$\Delta G = -\alpha_0(T_0 - T)P_3^2 + \alpha_{11}P_3^4 \quad (16)$$

It turns out that, even for the second order phase transitions leading to ferroelectric tetragonal phase the order parameter may attain only two directions ($\pm P_s$) correspondingly giving six domain states. Since the change in free energy density in a given phase is the same as revealed by equation (16), all domain states must be degenerate in terms of energy. The plot of Landau-type potential as function of polarization for proper ferroelectric second-order phase transition at different temperatures T is presented in Figure-3. The numerical solution indicates that, at higher temperatures ($T > T_0$) Landau energy density has one minimum at $P = 0$ and becomes broadened as the temperature decreases. Maximum broadening is observed to appear when $T = T_0$ but neither for $T > T_0$ nor at $T = T_0$ does the minimum go below$\Delta G = 0$.These observations imply that second-order phase transitions are continuous along the transition temperature with minima only at $\Delta G = 0$ for $T > T_0$ and at $\Delta G < 0$only when $T < T_0$.

In real systems, this corresponds to the fact that only a paraelectric cubic phase is stable for $T > T_0$such that equation (13) yields the solution of $P_3 = 0$and that the free energy density for cubic and tetragonal phase tends to equilibrium state as the temperature tends to the transition temperature value ($T \to T_0$) resulting to maximum broadening at $T = T_0$. For lower temperatures $T < T_0$ there are no cubic phase minima at $P_3 = 0$, instead two tetragonal minima at $\mp P$ and a maximum at $P = 0$are observed. As already introduced in preceding sections the observed two minima correspond to the up and down or rather right and left spontaneous tetragonal domain states (Figure-2). In this condition a material becomes ferroelectric with $P_3 = \mp P_S$with spontaneous polarization,P_S given by equation (15).

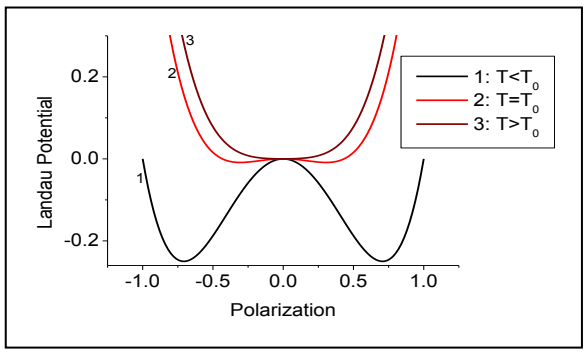

Figure-3. Landau-thermodynamic potential of the polarization for the ferroelectric second-order phase transition.

Second-order phase stability

The knowledge of correlations between the relative sizes of the Landau-type expansion coefficients constitute essential distinctive features towards the theoretical understanding of the nature of the equilibrium structures and configuration of second-order phase transitions occurring in materials of perovskite-type[16,17]. Taking a $BaTiO_3$-like model with second order phase transitions, Landau-type expansion simplifies to equation (17) which can be simplified further by minimizing it with respect to the polarization. Subsequently the polarization symmetries and their corresponding transformations are used in the determination of structural phase transitions and the associated phase stabilities for particular materials at given conditions.

$$\Delta G = \alpha_1(P_1^2 + P_2^2 + P_3^2) + \alpha_{11}(P_1^4 + P_2^4 + P_3^4) + \alpha_{12}(P_1^2P_2^2 + P_2^2P_3^2 + P_3^2P_1^2) \quad (17)$$

As already indicated in the previous sections, the solution of equation (17) describes the appearance of spontaneous polarization at $T < T_c$ and gives a non-polar parent phase characterized by net zero polarization states for$T > T_c$. It was observed (from the free energy density value of ferroelectric $BaTiO_3$ phases in equation 12) that for constant spontaneous polarizations equation (17) predicts minima at the points$(\mp P, 0, 0)$, $(0, \mp P, 0)$ and $(0, 0, \mp P)$ which correspond to the six tetragonal polarization states. The maxima are situated at points $(\mp P, \mp P, \mp P)$corresponding to the possible eight titanium displacement points in the rhombohedral phase. Thus, the two definite structural cases for perovskites of the barium titanite nature with second order phase transitions can be considered and these correspond to:

- Tetragonal phase with one of its polarization states arbitrary chosen such that$P_{Tet} = (0, 0, P_S)$. In this situation equation (17) changes to:

$$\Delta G = \alpha_1 P_S^2 + \alpha_{11} P_S^4 \quad (18a)$$

Energy density minimization gives:

$$P_S = \sqrt{\frac{-\alpha_1}{2\alpha_{11}}} \quad (18b)$$

- Rhombohedral phase with polarization states given as$P_{Rho} = (P_S, P_S, P_S)$ so that in this case equation (17) changes to:

$$\Delta G = 3\alpha_1 P_S^2 + 3\alpha_{11} P_S^4 + 3\alpha_{12} P_S^4 \quad (19a)$$

Energy density minimization gives:

$$P_S = \sqrt{\frac{-\alpha_1}{2(\alpha_{11}+\alpha_{12})}} \quad (19b)$$

Re-inspection of Curie-Weiss formula (equation 6) gives a straightforward evidence that the stiffness coefficient $\alpha_1$should depend on temperature in such a way that $\alpha_1(T > T_C) = \alpha_0(T - T_C)$ where$\alpha_0(> 0)$ is a constant. Second-order phase transition temperature, therefore, describes the critical temperature T_C at which the condition $\alpha_1(T_C) = 0$holds for any particular material. This implies that for the conditions$\alpha_1(T < T_C) < 0$ the cubic phase can no longer be stable and that below transition temperatures the structures of displacive ferroelectric perovskites are changed as a result of very small but cooperative atomic displacements. In fact these conditions are described also by equations (18) and (19), such that by neglecting the temperature dependence of the high-order stiffness coefficients α_{11} and α_{12}one arrives at two important cases, represented by equations (20) and (21). One observation revealed by equations (18 - 21) is that polarization depends on the relative values of α_{11} and α_{12} at given temperatures. This dependence has a strong influence on the structural phase transitions and constitutes relative stability details for the resultant second order phases.

$$P_S^{Tet}(T) = \sqrt{\frac{-\alpha_1(T)}{2\alpha_{11}}} = \sqrt{\frac{\alpha_0(T_C - T)}{2\alpha_{11}}} \quad (20)$$

$$P_S^{Rh}(T) = \sqrt{\frac{-\alpha_1(T)}{2(\alpha_{11}+\alpha_{12})}} = \sqrt{\frac{\alpha_0(T_C - T)}{2(\alpha_{11}+\alpha_{12})}} \quad (21)$$

From these equations, it is clear that:

$$(\alpha_{11}+\alpha_{12}) > 0 \quad (22)$$

When equation (22) is plotted for α_{12} (vertical) versus α_{11}(horizontal) a straight line relationshipwith line slope of negative one (-1) isobtained. The line separates the spacecoordinateintotwoequalregions of which the upper part is the feasibleregionsatisfyinginequality of equation (22). Other appropriate inequalities must be satisfied by the same high order Landau coefficients; for example it is also true from equations (18) and (20) that α_{11}must be positive ($\alpha_{11} > 0$). This becomes more apparent from Figure-4 when Landau-potential (equation 19) is plotted as function of polarization. Using the conditions $T < T_0$for$\alpha_{11} < 0$, the numerical solution obtained corresponds to the maximum of Landau energy density at$\Delta G = 0$. However, a monotonously decreasing series of free energy density is also observed. It appears that the minimum of the energy density is extending to infinity polarization$P_{min} \rightarrow \infty$value which is senseless and incorrect.Obviously, this situation entails that the conditions of$\alpha_{11} < 0$ for second-order phase transition is not a plausible one as it will imply that the tetragonal phase is no longer the stable phase of barium titanite. For comparison the numerical solution for $\alpha_{11} > 0$at the same temperature conditions is also shown in Figure-4. For this case the usual second order free energy minima at two states corresponding to $\pm P_S$are observed.

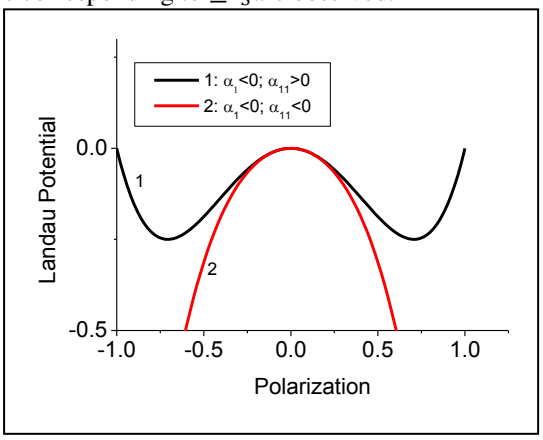

Figure-4. Second-order numerical solution of Landau functional for different signs of the coefficient α_{11}.

Assuming that all other suitable coefficient variations are satisfied such that during second order phase transition: (i) $\alpha_{12} > \alpha_{11}$for tetragonal phase and (ii) $\alpha_{11} > \alpha_{12}$for rhombohedral phase[17]. One finds that the minima of the Landau free-energy density for the second order phase can exist only inside the region defined by the following two inequalities: $\alpha_{11} > 0$and$(\alpha_{11} + \alpha_{12}) > 0$. It can be verified that these inequalities define the relative ranges of coefficients α_{11} and α_{12} leading to tetragonal and rhombohedral phase transformation boundaries. The transformations are easily visualized schematically from the model presented in Figure-5.From the model, it is observed that depending on the relative sizes of the high-order Landau-type free energy expansion coefficientsα_{11} and α_{12} one obtains a second-order phase transition either into a tetragonal or into a rhombohedral phase.

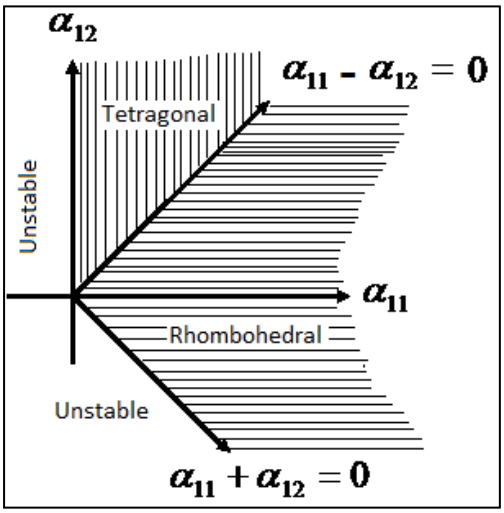

Figure-5. Relative ranges of high-order stiffness coefficientsα_{11} and α_{12} resulting to tetragonal and rhombohedral phases.

DOMAIN WALL IN FERROELECTRICS

The existence of domain structures in ferroelectric materials is often accompanied by substantial changes in the mechanical and electrical properties of materials[18]. As already indicated for the case of $BaTiO_3$, in order to understand these physical properties and all processes associated with domain phenomenon, one needs to go further down to the microscopic level so as to spot out how the atoms and sub-lattices move during domain formation and how those sub-lattices interact with each other. In order to do this, it is of primary essence to know the structure of the domain wall, its energy density, its spatial polarization profile and its corresponding distortions and stabilities.

Ferroelectric domain walls

Based on the Landau type theory some of domain-wall properties can be addressed, given that, the structural order parameter in the phenomenological functional is expected to change in the vicinity of the local regions of domain walls. These changes occurring in the structural order parameter turn out to be important theoretical problems for the analysis of the associated physical and phenomenological properties of domain walls[19-25]. For given domain structures, a ferroelectric domain wall represents a transition region that separates two ferroelectric domain states. Typically two major types of ferroelectric domain walls are known (Figure-6). The first one is the so-called 180° domain wall and the other option is the 90° walls. This implies that, upon transforming from cubic to ferroelectric phases, the resulting domain states in perovskites for example in tetragonal$BaTiO_3$-type can form any of the three structures, which are usually indicated by changes in the direction of order parameter. The possible three domain structures are:

- 180° wall, in which the polarizations in two domains have the same magnitude and axes but points in opposite directions to form a 180° domain wall.
- 90° wall, with charge-neutral domain wall in which the polarizations in the two domains are perpendicular to each other with head to tail configuration.
- 90° wall, with a charged domain wall for which the polarizations in the two domains are perpendicular with head-to-head or tail-to-tail configurations.

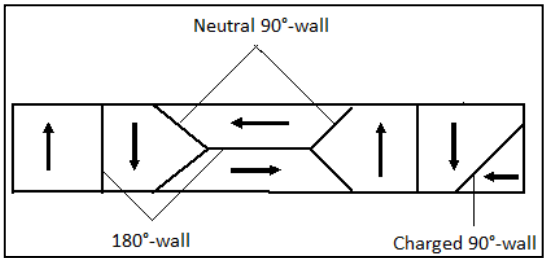

Figure-6. Illustration of 180° and 90°domain walls.

Since the preferred geometries of ferroelectric domain walls are known to follow from the wall energy considerations, it can be argued that only the 180°-wall and the head-to-tail 90° wall structures are prominently free of extra charges and so therefore stable since for their case according to equation (23):$div\ P = 0$. Note that equation (23) has been shown to account forthe stability or instability of domain walls in given materials[19-21]. Therefore, although it exists, the third 90° wall type with a charged domain wall is energetically unstable because of the additional Coulombic energy arising from the depolarizing fields as a result of charges in the wall.

$$div\ E_{depol} = [\varepsilon_b \varepsilon_0]^{-1}\ div\ P \tag{23}$$

Thus, equation (23) arises from the dipole-dipole interactions and becomes more important in the tail-to-tail or head-to-head 90° walls resulting to the instability of such walls. In the case of 180° and head-to-tail 90° walls the domains configurations are in such a way that the dipole arrangement attempts to reduce the energy due to non-uniform distribution of the polarizations which neutralize charges inside the domain wall region. In general there are various properties of domain walls[9]. To be certain only the domain wall width, its dependence on temperature and the spatial polarization profile for the case of cubic to tetragonal second order phase transition have been selected and considered for discussions in this paper. Starting with the Landau-type energy of domain wall an expression is developed in order to analytically estimate the magnitude of a ferroelectric domain-wall width, and numerically to show how domain wall width depends on temperature and finally the spatial distribution of polarizations inside a ferroelectric domain walls is derived in accordance with Landau theory.

Domain wall width

To begin with, one uses the conditions($\alpha_{11} > 0$, $\alpha_1 < 0$and $\alpha_{111} = 0$)of second-order to transform expression (2) such that the excess domain wall energy density for the proper ferroelectric perovskite in second-order phase transition can be written as in equation (24). Generally, a 180° domain wall is marked by inhomogeneous structure consisting of two energetically degenerate polarization states that results to energy disappearance in the vicinity of domain wall region. To avoid this problem the polarization gradient term is always included and is defined specifically by different materials order parameter gradients that can be determined by experiments such as soft phonon dispersion measurements[22,23].

$$\Delta G = -\alpha_1 P_z^2 + \alpha_{11} P_z^4 + \frac{1}{2} g_{44} \left(\frac{\partial P_z}{\partial x} \right)^2 \tag{24}$$

Since the domain wall follows from energy consideration, most of the general domain wall properties such as domain wall thickness can as well be expressed from the domain wall energy expression[24].It is already known from Figures 3 and 4 that the change in the Landau energy density is symmetric with respect to the$P_z = 0$

plane. This means that the net polarization at the centre of the domain wall isequal to zero ($P_z(x=0)=0$). Hence, the middle of the domain wall corresponds to the high temperature cubic structure of $BaTiO_3$.

Accordingly, from this observation one obtains the definition of the domain wall width associated to the polarization gradient inside the domain wall region[9]. Using the definition of the domain wall thickness from Hlinka and coworkers[24,26], the domain wall width2γ can be derived starting from the derivative of polarization component $P_Z$at the centre of the domain wall. This is given by:

$$2\gamma = 2\left[\frac{1}{P_S}\left(\frac{\partial P_z}{\partial x}\right)_{x=0}\right]^{-1} \quad (25)$$

In the case of 180° domain wall the analytical expression for domain wall energy barrier can be written. It is given by:

$$\Delta G_{Barrier} = \frac{1}{2} g_{44}\left(\frac{\partial P_z}{\partial x}\right)^2\Big|_{x=0} \quad (26)$$

The interpretation to equation (26) becomes apparent by stipulating that as one approaches the centre of the domain wall, $P_z \to 0$. This turns out to be the starting point for calculating the polarization gradient term. It is given by:

$$\frac{\partial P_z}{\partial x} = \sqrt{2\frac{\Delta G_{Barrier}}{g_{44}}} \quad (27)$$

Combining equations (26) and (27) readily gives the expression relating the width of a 180° domain wall to the energy barrier. It is given by:

$$t_w = 2\gamma_{180^0} = P_S\sqrt{\frac{2g_{44}}{\Delta G_{Barrier}}} \quad (28)$$

The energy barrier, $\Delta G_{Barrier}$ forthe formation of 180° domain that appears in equation (28) arise from the tendencies of increasing Landau free energy density when approaching thedomain wall[24]and it is not affected by polarization gradient term[9]. This means that $\Delta G_{Barrier}$ can be defined alternatively by the homogeneous polarization states when$P_Z = P_S$. Hence, the energy barrier $\Delta G_{Barrier}^{180^o}$can be expressed solely through the parameters of the Landau free energy parameters. Thus, using$\Delta G_{Barrier}^{180^o} = -\alpha_1 P_S^2 + \alpha_{11} P_S^4$with spontaneous polarization P_s given by $P_S^2 = \alpha_1/2\alpha_{11}$into (28) the energy barrier and the corresponding domain wall width are readily obtained. This procedure leads to:

$$\Delta G_{Barrier}^{180^0} = \frac{-\alpha_1^2}{4\alpha_{11}} \quad (29a)$$

and

$$t_w = 2\gamma_{180^0} = \sqrt{\frac{-4g_{44}}{\alpha_1}} \quad (29b)$$

Where $\gamma_{180^o} = 0.5t_w = \sqrt{-g_{44}/\alpha_1}$is the spatial domain wall correlation length which is equivalent to half the domain wall width.

For the case of $BaTiO_3$, $g_{44} = 2\times10^{-11}\text{Jm}^3\text{C}^{-2}$[21] while at room temperature$\alpha_1 = -3.006\times10^7\text{JmC}^{-2}$ (Table-3). When these values are inserted into (29b), the domain wall-width of t_w = 1.63 nm(16.3Å) is obtained. It was suggested in earlier studies that the experimental domain wall thickness in $BaTiO_3$is of the order between 10 and 40 Å[18]. This value is in good agreement with domain wall thickness obtained in the present calculation.

Dependence of domain wall width on temperature

In order to introduce the variations of domain wall thickness with temperature, the Curie-Weiss law is used. The stiffness coefficient α_1 is replaced by$\alpha_1(T > T_C) = \alpha_0(T - T_C)$. This leads to the temperature dependence of a domain wall width equation. It is given by:

$$2\gamma_{180^0} = \sqrt{\frac{4g_{44}}{\alpha_0(T_C - T)}} \quad (30)$$

The numerical solution of equation (30) for the case of $BaTiO_3$-type perovskite materials is presented in Figure-7. The indexed characteristic parameters are for $BaTiO_3$that were used in equation (30) to arrive at the plot. The solution predicts an increase of domain wall width with increasing temperature until a maximum width is attained at $T = T_C$. This domain wall behavior are in agreement with ferroelectric domain-wall width variation with temperature that were reported earlier from experiments by Dennis and Bradt [27].

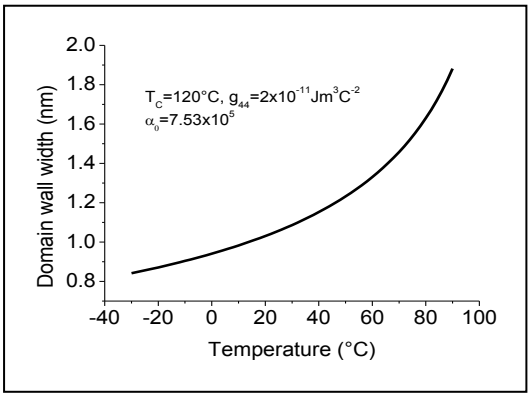

Figure-7. Dependence of ferroelectric $BaTiO_3$domain wall thickness on temperature.

Domain wall profile

Starting with Landau energy density of a given sample system, *f:*

$$f = -\alpha_1 P_z^2 + \alpha_{11} P_z^4 + \frac{1}{2} g_{44} \left(\frac{\partial P_z}{\partial x} \right)^2 \quad (31)$$

Thetotal free energy G of the system is obtained by integrating *f*. This leads to:

$$G = A \int_{-\infty}^{\infty} f(P_z, P_z', x) dx = A \int_{-\infty}^{\infty} \left(-\alpha_1 P_z^2 + \alpha_{11} P_z^4 + \frac{1}{2} g_{44} \left(\frac{\partial P_z}{\partial x} \right)^2 \right) dx \quad (32)$$

where A is the cross-sectional area of the sample. The spatial distribution of polarization, $P_Z(x)$inside the domain wall should minimize the total free energy of the system[9]. Therefore, in order to see the polarization profile inside the domain wall one has to find where the total energy G attains its minimum value. Equation (32) is an indefinite integral; its minimization goes through a number of steps discussed:

- To state the problem: given a function$f(P_Z, P_Z', x)$, where$P_Z' = dP_Z/dx$; and needed to find$P_Z(x)$such that equation (32) is minimized. To find the minimum of the integral in (32) one needs to derive the Euler-Lagrange differential equation. First, as illustrated in Figure 8, one lets the true polarization profile, the one such that G is minimized to be represented byP_Z^{min}. Then, if there exists any arbitrary function say*P(x)*and assuming a neutral domain wall, G will increase since the new polarization at any given points along the profile will now be determined from

$$P_z(x) = P_z^{\min}(x) + P(x) \quad (33)$$

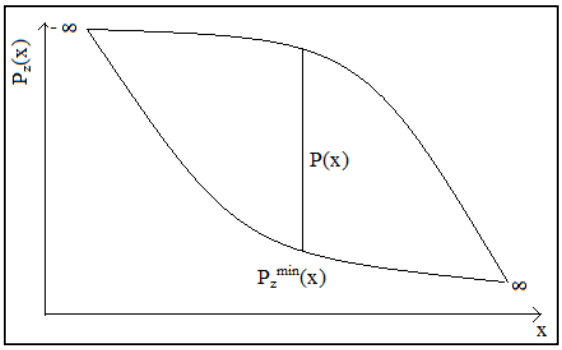

Figure-8. Schematic illustration of the change that can occur in the polarization profile of a neutral domain wall because of adding an arbitrary function *P(x)*.

- Since the integral needs to be minimum at the polarization profile defined by$P_Z^{min}(x)$, one needs to find how much larger does the integralgets because of the added, however small, values of*P(x)*. This is readily obtained from *f* which is a function of two variables such that equation (34) gives the increase in the integral at any arbitrary selected point along the polarization profile.

$$\frac{\partial f}{\partial P_z} P(x) + \frac{\partial f}{\partial P_z'} P'(x) \quad (34)$$

- The first term of equation (34) tells how much larger the integral gets when an amount of *P(x)* is added, and the second one explains how much bigger it gets because of adding$P'(x)$. The total change in energy denoted as δGisobtainedfrom the change in each point integrated over the all polarization profile. It is given by:

$$\delta G = \int_{-\infty}^{\infty} \left[\frac{\partial f}{\partial P_z} P(x) + \frac{\partial f}{\partial P_z'} P'(x) \right] dx \quad (35)$$

- For the true polarization profile with any arbitrary small increase of *P(x)*and$P'(x)$, the total change in energy of the system has to be zero ($\delta G = 0$). This is a static condition meaning that equation (35) can be rewritten as:

$$\int_{-\infty}^{\infty} \left[\frac{\partial f}{\partial P_z} P(x) + \frac{\partial f}{\partial P_z'} P'(x) \right] dx = 0 \quad (36)$$

- Equation (36) defines a condition from which *f* can be manipulated. A closer look at the same equation (36) indicates that the best way of starting its manipulation is to simplify the second term inside the bracket of the integral. It is given by:

$$\frac{d}{dx}\left(\frac{\partial f}{\partial P_z'} P(x) \right) = \frac{\partial f}{\partial P_z'} P'(x) + \frac{d}{dx} \frac{\partial f}{\partial P_z'} P(x) \quad (37a)$$

- Or equivalently as,

$$\frac{\partial f}{\partial P_z'} P'(x) = \frac{d}{dx}\left(\frac{\partial f}{\partial P_z'} P(x) \right) - \frac{d}{dx} \frac{\partial f}{\partial P_z'} P(x) \quad (37b)$$

- The left hand term of equation (37b) can be inserted back into the integral but now replacing it with the equivalent right hand terms of (37b) and equation (36) changes to:

$$\int_{-\infty}^{\infty} \left[\frac{\partial f}{\partial P_z} P(x) + \frac{d}{dx}\left(\frac{\partial f}{\partial P_z'} P(x) \right) - \frac{d}{dx}\left(\frac{\partial f}{\partial P_z'} \right) P(x) \right] dx = 0 \quad (38a)$$

- Or rearrangement to,

$$\int_{-\infty}^{\infty} \left[\frac{\partial f}{\partial P_z} - \frac{d}{dx}\left(\frac{\partial f}{\partial P_z'} \right) \right] P(x) dx + \int_{-\infty}^{\infty} \frac{d}{dx}\left(\frac{\partial f}{\partial P_z'} P(x) \right) dx = 0 \quad (38b)$$

- Integration of the second term in equation (38b) results to:

$$\int_{-\infty}^{\infty} \frac{d}{dx}\left(\frac{\partial f}{\partial P_z'} P(x)\right) dx = \frac{df}{dP_z'} P(x)\Big|_{-\infty}^{\infty} \quad (39)$$

- Because the system is either starting or ending at the endpoints of the polarization profiles there is no effects of polarization variations. Such a condition is written as:

$$P(-\infty) = P(\infty) = 0 \quad (40)$$

- That is to say, since $-\infty$ and ∞ define the twoendpoints of the system (Figure-8), *P(x)* in equation (39)would mean for the endpoints polarization variation and it turns out to be zero according to equation (40).This way, the whole equation(39) reduces to:

$$\int_{-\infty}^{\infty}\left[\frac{\partial f}{\partial P_z} - \frac{d}{dx}\left(\frac{\partial f}{\partial P_z'}\right)\right] P(x)dx = 0 \quad (41)$$

- Equation (41) can be interpreted as follows, for a physical system at equilibrium, the requirement of minimum energy is in such a way that the total change in energy of the system, δG must vanish for any infinitesimally small change in *P(x)*. Now, since for any arbitrary small change in the function *P(x)*the integral need to be zero at all points for the polarization profile of $P_Z^{min}(x)$, it turns out that the solution of equation (41) leads to:

$$\left[\frac{\partial f}{\partial P_z} - \frac{d}{dx}\left(\frac{\partial f}{\partial P_z'}\right)\right] = 0 \quad (42)$$

- In order to obtain the two terms in this equation (42), one recalls back the energy density function *f*from equation (31). When this is taken into account the two terms are given by:

$$\frac{\partial f}{\partial P_z} = -2\alpha_1 P_z + 4\alpha_{11} P_z^3 \quad (43)$$

$$\frac{d}{dx}\left(\frac{\partial f}{\partial P_z'}\right) = g_{44}\frac{d}{dx}P_z' = g_{44}\frac{d^2 P_z}{dx^2} \quad (44)$$

- These lead to:

$$-2\alpha_1 P_z + 4\alpha_{11} P_z^3 + g_{44}\frac{d^2 P_z}{dx^2} = 0 \quad (45)$$

- Equation (45) has a form of nonlinear second-order differential equation whose solution satisfies the boundary conditions: $P_Z \to P_S$ for $x \to \infty$ and $P_Z \to -P_S$for $x \to -\infty$[9]. It is given by :

$$P_z(x) = P_S \tanh\left(\frac{x}{\sqrt{-g_{44}/\alpha_1}}\right) = P_S \tanh\left(\frac{x}{\gamma_{180^\circ}}\right) \quad (46)$$

Thus in a given sample system the free energy can vary continuously in space. As a consequence the spatial distributions of polarization, $P_Z(x)$tends to minimize the total energy of the sample by continuously enlarging*x*and consequently lowering the polarization gradient term. This way the most stable patterns that correspond to the minimum of the total free energy of the sample are such that$x = \mp\infty$. These requirements are usually stipulated as boundary conditions stating as above[9]. The numerical spatial solution for polarizations inside the domain wall turns out to be as shown in Figure-9. The profile shows a continuous kink-type variation of polarization states inside of a 180° domain wall reaching zero value at the centre of the wall. This indicates that, 180° domain walls appear to be connecting the two $(0, 0, +P_s)$ and $(0, 0, -P_s)$ domain states at $x = 0$. The polarization profile also shows that the polarizations reach their symmetric absolute value at approximately the same distance from the middle of the domain wall as P_Z returns to the bulk polarization values.

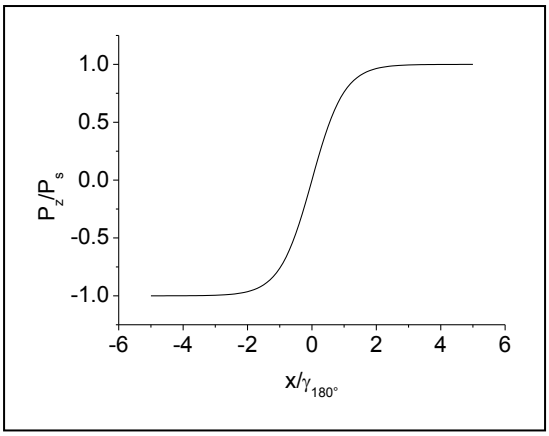

Figure-9. Illustration of normalized spatial polarization profile across a 180° domain wall in perovskite of $BaTiO_3$-type with second order phase transition at room-temperature. 180° domain wall is marked by inhomogeneous structure of polarizations consisting of two neighboring polarization states which are energetically degenerate. The polarization states are situated in the two neighboring domains whose tetragonal axes are the same but point in opposite direction with 180° out of phase.

CONCLUSIONS

This paper presents the results of Landau type phenomenological theory for some selected properties of domains and domain walls in ferroics. The study was mainly devoted to perovskite ferroelectrics. Two types of temperature induced phases have been distinguished: first order and the continuous second order phase transitions.

Contrary to first order phase transitions, in second order transitions the change is gradual until the transition temperature and only one phase exists at each temperature including the transition point. The stability of ferroelectric phases of a $BaTiO_3$type material was compared at room temperature and tetragonal phase was found to be the stable phase. The number of domains states for the three states were calculated and confirmed to be 6for tetragonal, 12 for orthorhombic and 8 for rhombohedral. The calculation of domain wall thickness in tetragonal $BaTiO_3$at room temperature showed that it is in the order of 16.3 Å. Analytical and numerical solutions of ferroelectric domain wall profile and of how domain wall thickness depends on temperature were successfully developed.It was found that Landau phenomenological theory of ferroelectricsis very well established and interesting thermodynamic treatments have been done including estimations of the Landau type expansion coefficients. This made it possible to simplify the Landau type functional equations and use them to establish room temperature spontaneous polarization in $BaTiO_3$; it is of the order of 0.26 Cm^{-2}. However, it could be amenable if both experimental and theoretical studies would be carried out together in order to compare the experimental data with theoretical findings presented. This would answer many of unresolved open problems and difficulty that are usually encountered when two or several experimental results for Ferroelectricity and various phase transitions occurring in ferroelectric ferroics are compared.

REFERENCES

[1] T. Y. Hsu, Q. P. Meng, Y. H. Rong and X. J. Jin. 2005. Perspective in Application of the Phase Field Theoryto Smart Materials Performance. Materials science forum.475-479: 1909-1914.

[2] J. C. Tolédano and P. Tolédano.1987.The Landau Theory of Phase Transitions, Singapore: World Scientific Publishing Co. Pte.

[3] K. Yokoh, S.-M. Nam, H. Kakemoto, T. Tsurumi, H. Kumagai and S. Wada. 2006. Domain Wall Engineering in Potassium Niobate Single Crystals and Their Piezoelectric Properties. Key engineering Materials. 320: 147-150.

[4] A. S. Bhalla, G. Raina and S. K. Sharma.1998.Felloelasticsticdomainstudy by atomic force microscope (AFM). Materials Letters. 35: 28-32.

[5] S. Wada, K. Yako, T. Muraishi, H. Kakemoto and T. Tsurumi. 2006. Development of Lead-free Piezoelectric Materials using Domain wall engineering. Key Engineering Materials. 320: 151-154.

[6] S. Wada, K. Yako, H. Kakemoto, J. Erhart and T. Tsurumi. 2004. Enhanced Piezoelectric Property of $BaTiO_3$ Single Crystals with different Domain Sizes.Key engineering Materials. 269: 19-22.

[7] K. Yako, H. Kakemoto, T. Tsurumi and S. Wada.2006. Enhanced Piezoelectric properties of Barium Titanate Single Crystals by Domain Engineering. Key Engineering Materials. 301: 23-26.

[8] B. A. Strukov and A. P. Levanyuk. 1998. Ferroelectric Phenomena in Crystals; Physical Foundation, Springer.

[9] A. K. Tagantsev, L. E. Cross and J. Fousek.2010. Domains in Ferroic Crystals and thin Films, New York: Springer.

[10] M. J.Haun, E. Furman, S. J. Jang, H. A. McKinstry and L. E. Cross. 1987. Thermodynamic theory of $PbTi0_3$. J. Appl. Phys. 62(8): 3331-3338.

[11] A. J. Bell. 2001. Phenomenologicallyderivedelectricfield-temperature phase diagrams and piezoelectric coefficients for single crystal barium titanate under fields along different axes. Applied physics. 89(7): 3907-3914.

[12] Y. L. Li, L. E. Cross and L. Q. Chen.2005. A phenomenological thermodynamic potential for $BaTiO_3$ single crystals. Appl. Phys. 98: 064101-1-4.

[13] A. S. Sidorov. 2004. Structure of inorganic compounds; Specific features of structure and ferroelectric properties of $BaTiO_3$ phases. Crystallography reports. 49(49): 619-625.

[14] Y. L. Wang, A. K. Tagantsev, D. Damjanovic and N. Setter.2006. Anharmonicity of $BaTiO_3$ single crystals. Phys. Rev. B. 73: 132103.

[15] J. C. Johson.1965.Somedielectric and electro-optic properties of $BaTiO_3$ single crystals. AppliedPhysicsLetters. 7(7): 221-223.

[16] J. C. Slonczewski and H. Thomas.1970. Interaction of elasticstrain with the structural transition of strontium titanate. Phys. Rev. B. 1: 3599.

[17] A. K. Tagantsev, E. Courtens and L. Arzel. 2001. Prediction of a low temperature ferroelectric instability in antiphase domain boundaries of strontium titanite. Phys. Rev. B. 64: 5.

[18] E. K. W. Gao, R. K. Mishra and G. Thomas. 1981. Electron microscopy study of the ferroelectric domains and domain wall structure in $PbZr_{0.52}Ti_{0.48}O_3$. Appl. Phys. 52: 2944.

[19] Y. Ishibashi and E. Salje. 2002. A theory of ferroelectric 90 degree domain wall. Phys. Soc. Jpn. 71(11): 2800-2803.

[20] J. Hlinka. 2008. Domain Walls of $BaTiO_3$ and $PbTiO_3$withinGinzburg-Landau-Devonshire mode. Ferroelectrics. 375: 132-137.

[21] J. Hlinka and P. Màrton. 2006. Phenomenological model of a 90° domain wall in $BaTiO_3$-type ferroelectrics. Phys. Rev. B. 74: 104104.

[22] W. Cao and G. R. Barsch. 1990. Landau-Ginzburg model of inter phase boundaries in improper ferroelasticperovskites of symmetry. Phys. Rev. B. 41(7): 4334.

[23] W. Cao. 1994. Polarization gradient coefficients and the dispersion surface of the soft mode in perovskiteferro electrics. J. Phys. Soc. Jpn. 63(3): 1156-1161.

[24] Y. Ishibashi. 1993. The 90°-Wall in the tetragonal phase of $BaTiO_3$-type ferroelectrics. Phys. Soc. Jpn. 62(3): 1044-1047.

[25] W. Cao and L. E. Cross.1991. Theory of tetragonaltwin structures in ferroelectric perovskites with a first-order phase transition. Phys. Rev. 44(1): 5-12.

[26] J. Padilla, W. Zhong and D. Vanderbilt. 1996. First-principles investigation of 180° domainwalls in $BaTiO_3$. Phys. Rev. B. 53: R5969–R5973.

[27] M. D. Dennis and R. C. Bradt. 1974. Thickness of 90° ferroelectric domain walls in $(Ba,Pb)TiO_3$ single crystals. Appl. Phys. 45: 1931.